Energy Conversion and Management 78 (2014) 825–834

Contents lists available at ScienceDirect

Energy Conversion and Management

journal homepage: www.elsevier.com/locate/enconman

Predictive direct power control for photovoltaic grid connected system: An approach based on multilevel converters

Kamel Barra *, Djamel Rahem

Larbi Ben M'hidi University, Oum El Bouaghi 04000, Algeria

ARTICLE INFO

Article history:
Available online 23 October 2013

Keywords:
Photovoltaic grid conversion chain
Predictive control
Finite states-space model
Cost function
Multilevel converter

ABSTRACT

The paper presents an improved predictive power control for a photovoltaic conversion chain connected to a grid based on finite states space model of the converter. The proposed control algorithm selects the switching state of the inverter that minimizes the error between active and reactive power predictions to their computed values for all different voltage vectors. The optimal voltage vector that minimizes a cost function is then applied to the output of the power converter. Once the proposed predictive strategy is validated, a multilevel converter is then used to improve and highlight the obtained results. The proposed predictive control strategy uses only one sample time prediction and it is very intuitive since it is very simple and provides best performances compared to other modulation techniques.

1. Introduction

Photovoltaic (PV) energy offers an environmentally friends source of electricity and considered as the most promising source of energy which the fuel is sunshine, renewable, without pollution, abundant and broadly available. The PV energy applications can be divided into two categories, namely: (1) stand alone systems (water pumping, domestic and street lighting, electric vehicles, military and space applications) requiring storage batteries suitable for low power systems. (2) Grid connected systems (hybrid systems, power plants) which does not requiring storage batteries and used for medium and high power applications [1-9].

Grid connected PV system consists of a series/parallel connection array of PV panels connected to a power conditioning system stage which is responsible for the proper transfer of the energy produced by PV array to the grid generally via a DC/DC converter that used as a MPPT controller and an inverter that converts the DC voltage to a single or three-phase AC voltage and at last a AC filter that absorbs voltage/current harmonics due to switching functions [10-14].

Due to nonlinear *I–V* characteristics of photovoltaic cells, a maximum power point tracking algorithm MPPT is adopted to extract maximum output power to the environmental changes such as solar insulation, temperature and load variations. Among the two last decades, several algorithms have been developed and addressed in many literatures in order to achieve maximum power point tracker, these techniques vary between them in many aspects, including simplicity, convergence speed, hardware implementation, sensors required, cost, range of effectiveness and need for parameterization. The most classical methods commonly used are Perturb and Observe (P&O), Incremental Conductance (IncCond), Hill Climbing (HC) and Open/Short circuit methods [2–4]. Note that the MPPT methods based artificial intelligence (MPPT based fuzzy logic and neural network), robust MPPT using sliding mode controller are not cited here.

Model Predictive Control (MPC) is a very powerful control strategy that uses the model of the system to precalculate the behavior of the system for a predefined horizon in the future. A cost function evaluates the precalculated results and determines the optimal future control actions. Generalized Predictive Control (GPC) is the most popular method of MPC family methods since it can be applied to a great variety of systems where dead times can be easily compensated, the concept is very intuitive and easy to understand, the multivariable case can be easily considered, easy inclusion of non-linearities in the model. The main disadvantages of the GPC control is the large amount of calculations, compared to classic controllers and the direct influence of the model on the quality of the resulting controller.

Recently, Finite States Model Predictive Control (FS-MPC) appears as an attractive alternative and offers a completely different and powerful approach to control power converters due to its fast dynamic response, no need for linear controllers, no need for modulator (PWM or SVM), completely different approach compared to PWM, extremely simple, very good performance and can be implemented with standard commercial microprocessors. The method is based on the fact that a finite number of possible switching states can be generated by power converter (7 states for a two levels three-phase inverter, 27 states for a three levels, 64 states for a four

* Corresponding author.
E-mail addresses: barakamel@yahoo.fr (K. Barra), rahem_djamel@yahoo.fr (D. Rahem).

0196-8904/$ - see front matter © 2013 Elsevier Ltd. All rights reserved.
http://dx.doi.org/10.1016/j.enconman.2013.06.064

levels,...) and that the model of the system can be used to predict the behaviour of the variables for each switching state. For the selection of the appropriate switching state to be applied to the system a quality function must be defined. The cost function is then evaluated for the predicted values on each sampling interval and the optimal switching state that minimizes the quality function is selected to apply during the next sampling interval [15–18].

The paper presents a simple method to control a photovoltaic conversion chain connected to a three phase AC grid. The method uses at first a predictive control associated with a two-level three phase voltage source inverter to validate the control strategy, then a three-level inverter is used to improve and highlight the results. The paper is organized as follows. Section 2 is dedicated to the modelling framework of the considered PV array. Section 3 presents the modified Incremental Conductance MPPT algorithm. Section 4 models a two level voltage source inverter before its inclusion in the predictive power control well explained in Section 5, while the results are presented and commented in Section 6 followed by the predictive power control associated to a three-level converter in Section 7 and finally a conclusion is given in the last Section 8.

2. PV modeling

The mathematical model of a solar cell composed of a light generated current source, diode, series and parallel resistance is given for the output current, photocurrent and PV saturation current by [9]:

$$I_{PV} = I_{ph} - I_d\left[\exp\left(\frac{q}{K_b TA}V_{PV}\right) - 1\right] \quad (1)$$

$$I_{ph} = S(I_{scr} + k_i(T - T_r)) \quad (2)$$

$$I_d = I_{rr}\left(\frac{T}{T_r}\right)^3 \exp\left(\frac{qE_g}{kQA}\left[\frac{1}{T_r} - \frac{1}{T}\right]\right) \quad (3)$$

where I_{PV}, V_{PV} is the output current and voltage (A, V), T is cell temperature (K), S is solar irradiance (W/m^2), I_{ph} is light generated current, I_d is PV saturation current, I_{rr} is saturation current at T_r, I_{scr} short circuit current at reference condition, T_r is reference temperature, q is charge of an electron, k_b is the Boltzmann's constant.

The PV panel considered here is a typical MSX60-60W PV module. Figures from Figs. 1–4 illustrate a 3D plot of the I–V and P–V characteristics for different insulation and temperature levels. On these curves, one can see that the characteristics are nonlinear and are crucially influenced by solar radiations and temperature variations.

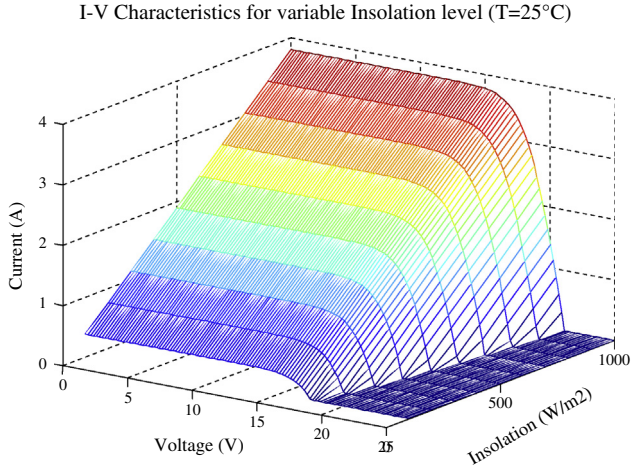

Fig. 1. 3D plot of I–V characteristics for different irradiance levels.

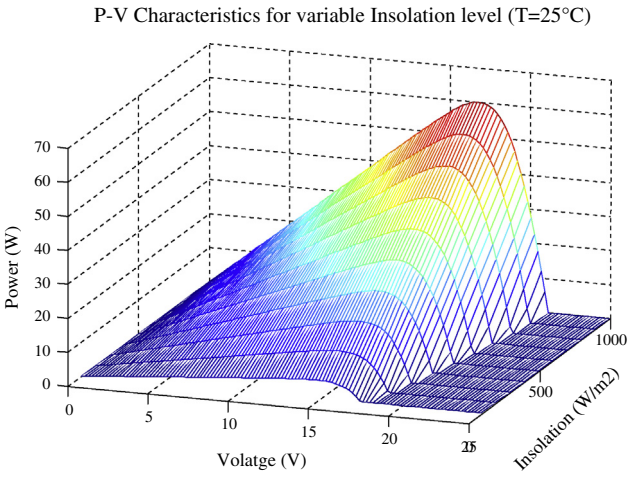

Fig. 2. 3D plot of P–V characteristics for different irradiance levels.

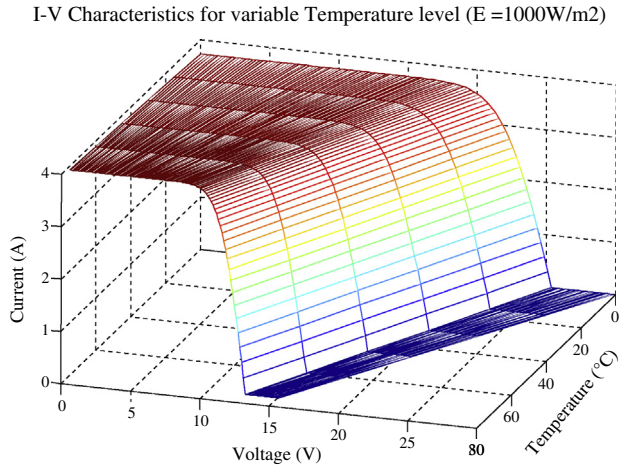

Fig. 3. 3D plot of I–V characteristics with temperature effect.

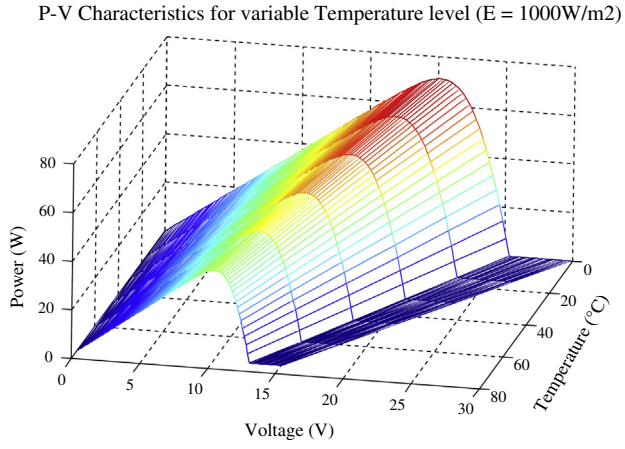

Fig. 4. 3D plot of P–V characteristics with temperature effect.

3. MPPT algorithm

Consider a photovoltaic grid conversion chain composed of a PV array, a two-level three phase voltage source inverter VSI, a R-L filter and a three phase symmetric electric grid as illustrated by Fig. 5.

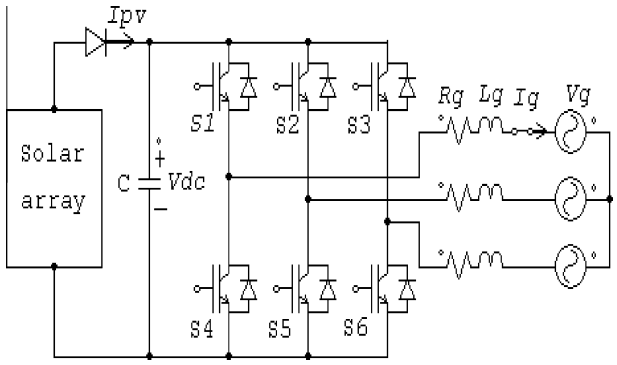

Fig. 5. Configuration of the studied system.

Due to their low efficiency, PV systems should be designed to operate always at their maximum output power level.

The (P&O) method is the most widely used in commercial PV products, where the algorithm is considered as "trial and error" method [4]. The MPPT increases PV output power by a small amount and then detects the actual output power. If the output power indeed increased, it will increase again until the output power starts to decrease, at which the controller decreases the reference to avoid collapse of the PV output. The main advantage of the method is the simplicity control structure yielding easiness implementation but it presents some drawbacks such as slow trial and error process, oscillations in steady state around MPP sunshine condition leading fluctuating inverter output and the method may fail to track the maximum power point due to sudden changes in sunshine.

Climbing Hill method (HC) is based on the relationship between the power of the panel and the value of the duty cycle D, mathematically, the MPP is reached when dP_{PV}/dD is forced to zero by the command. Periodically, the power P_{PVn} is compared to the value previously determined P_{PVn-1}, depending on the result of the comparison, the sign of the slope value changes or stays the same. This has the effect of increment or decrement the value of the duty cycle. Once the MPP is reached, the system oscillates around it indefinitely, so joining the trade-off between speed and accuracy.

The Incremental Conductance Algorithm (IncCond) is based on the fact that the MPP is reached when the ratio $dP/dV = 0$, the operating point is located (left/right) according to the sign of the above ratio and the MPP is tracked more accurately than in (P&O) method by comparing Incremental Conductance and instantaneous conductance dI_{PV}/dV_{PV} of a PV array to avoid the problem of oscillation because it stops perturbing the operating point when the reference voltage reaches the maximum power point voltage. However, it has the disadvantage of possible output instability due to the use of derivative algorithm, also the differentiation process under low levels of irradiance becomes difficult and consequently the results are unsatisfactory. In previous ccomparative studies (Kuo et al., 2001; Hussein et al., 1995; Yu et al., 2004), it has been shown that (IncCond) tracks fast the maximum power point (MPP) under rapid changing atmospheric conditions. The traditional Incremental Conductance method uses a fixed iteration step size.

A large step size contributes to faster dynamics of the extracted power but causes oscillations in current, voltage and power, also a small step size reduces the oscillations but produces a slower dynamics of the drawn power. As a compromise, a modified Incremental Conductance algorithm with a variable iteration step size is applied.

The step size is automatically tuned according to operating point. If the operating point is far from MPP, the algorithm increases the step size which enables a fast tracking ability. If the operation point is near to the MPP, the step size becomes automatically very small that the oscillations are well reduced. The variable step size adopted for this algorithm is given by the following equation [7]:

$$d = \lambda \left| \frac{Vpv(k)Ipv(k) - Vpv(k-1)Ipv(k-1)}{Vpv(k) - Vpv(k-1)} \right| \tag{4}$$

where $Vpv(k), Ipv(k)$ are the output voltage and current of the PV array at the kth sample of time, λ is the scaling factor for adjusting the step size.

The simulation performances of the two methods are shown in Fig. 6 for fixed iteration step size and by Fig. 7 for modified step size where it is easy to see that the modified step size method gives best performances in front of sudden changes of irradiation.

More MPPT algorithms are addressed in previous works such as: Modified P&O, Three Point Weight Comparison (Hsiao et al., 2002), Constant Voltage (CV) (Yu et al., 2002), IC and CV combined (Yu et al., 2002), Short Current Pulse (Noguchi et al., 2002), Open

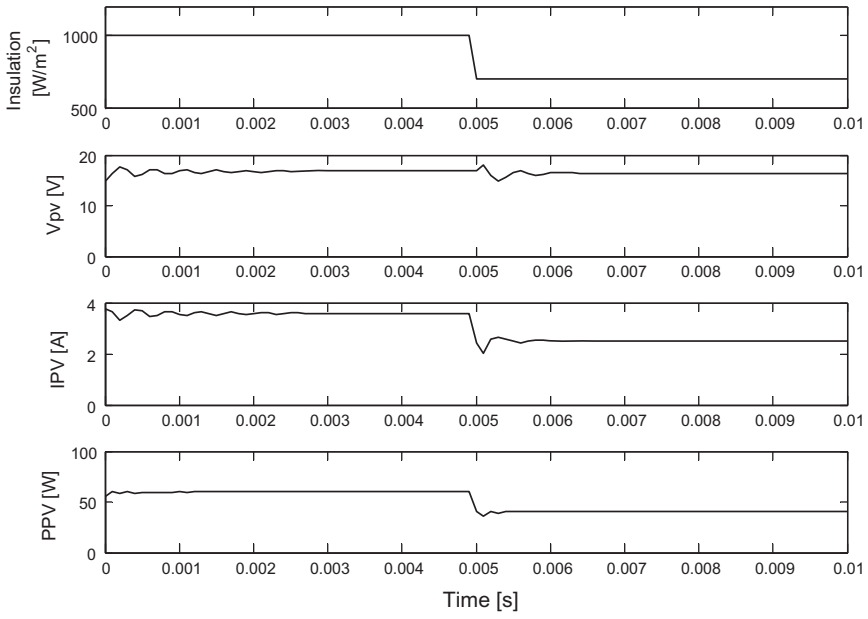

Fig. 6. Incremental Conductance MPPT algorithm performance with fixed iteration step size.

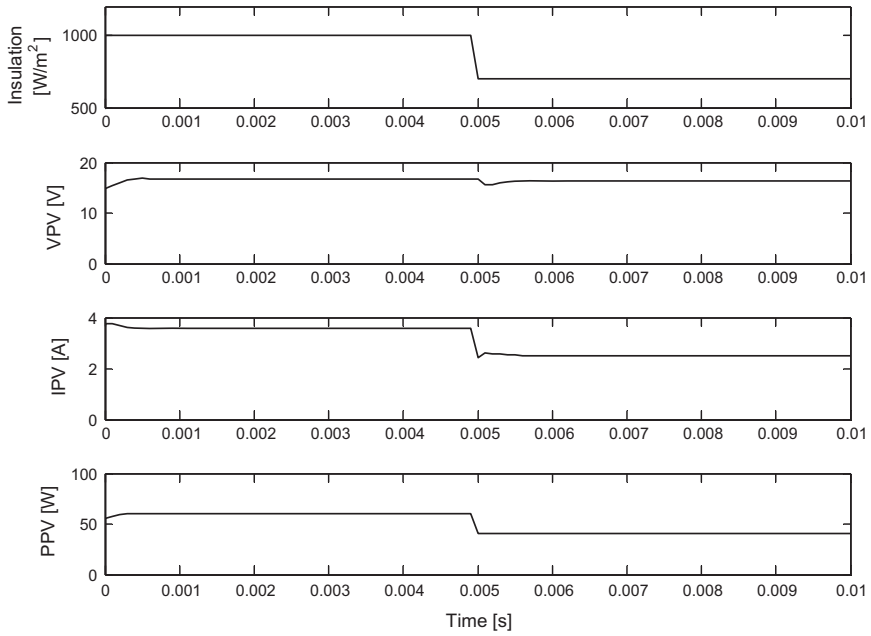

Fig. 7. Incremental Conductance MPPT algorithm with variable step size.

Circuit Voltage (Lee et al. 2003), the Temperature Method (Park et al., 2004) and methods derived from it. These techniques are easily implemented and have been widely adopted for low-cost applications [9].

4. Two level voltage source inverter model

To describe the inverter output voltages, the concept of complex space vector is applied. For a two level voltage source inverter feeding a symmetrical three-phase grid connected system given in Fig. 5, each leg is composed of two by-directional switches (S_{i1}, S_{i2} $i = a, b, c$) where a, b, c the three phases. The switching states S determined by gating signals are given in vectorial form as follows [15–18]:

$$S = \frac{2}{3}(S_a + aS_b + a^2S_c) \tag{5}$$

where $a = e^{j2\pi/3}$. S_i takes the value of 0 if S_{i1} is off and S_{i2} is on, S_i takes the value of 1 if S_{i1} is on and S_{i2} is off.

The output voltage space vectors of the inverter are:

$$V = \frac{2}{3}(v_{aN} + a\,v_{bN} + a^2\,v_{cN}) \tag{6}$$

(v_{aN}, v_{bN}, v_{cN}): are the phase to neutral (N) voltages.

As it is well known, there are eight possible voltage vectors that the inverter can apply to the grid terminals. By using these switching functions the grid space voltage vector can be expressed as:

$$V(S_a, S_b, S_c) = \sqrt{\frac{2}{3}}V_{dc}(S_a + S_b e^{j2\pi/3} + S_c e^{j4\pi/3}) \tag{7}$$

where V_{dc} is the DC-link voltage.

According to the combinations of switching modes, the space vectors V_7 (0,0,0) and V_8 (1,1,1) are the space zero voltage vectors and the others are the space nonzero active voltage vectors as shown in Fig. 8.

Also, the inverter output voltage is related to DC link voltage by:

$$V = V_{dc}S \tag{8}$$

The inverter output voltage vector is kept constant during the switching period, so the inverter current and, hence, the grid currents can be controlled by choosing the appropriate voltage vector.

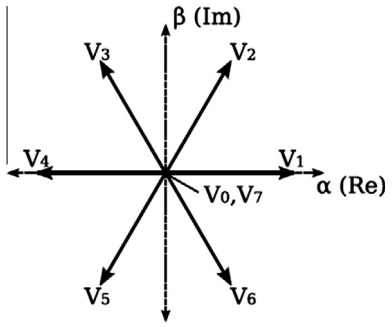

Fig. 8. Representation of different voltage vectors of a two level voltage inverter.

5. Predictive power control

Standard control scheme for a three phase grid connected photovoltaic system is given by Fig. 9. The system is typically composed of a PV array that converts solar energy to electric energy, an MPPT algorithm to track the MPP, a three phase DC–AC voltage inverter that converts DC to AC voltage, an AC filter that absorbs voltage/current harmonics generated by inverter and finally a grid utility.

The main objectives to be fulfilled in order to transfer efficiently the solar energy to the utility grid are:

- To track efficiently the MPP.
- To obtain unity power factor in the grid side.
- To provide low harmonic distortion at the output (THD < 4.6%).

To do that, an improved predictive power control scheme is proposed in Fig. 10. The main blocs of the proposed predictive power control are explained below.

5.1. Predictive model

For a two-level voltage source inverter, the finite set of states of the switches S_1, …, S_6 contains only seven different voltage vectors

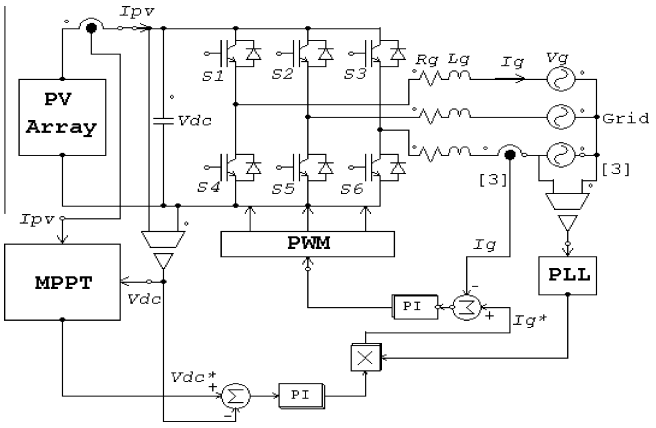

Fig. 9. Standard control scheme for a three phase grid connected photovoltaic system.

and the dynamics of the grid current I_g can be expressed by the vector equation:

$$V_{[3]} = R_g I_{g[3]} + L_g \frac{dI_{g[3]}}{dt} + V_{g[3]} \tag{9}$$

where V is the output voltage space vectors generated by the inverter and R_g, L_g are respectively the resistance and inductance per phase of the grid filter and V_g is a balanced three phase grid voltage vector assumed to be sinusoidal with constant frequency and constant amplitude.

By approximating the derivative $\frac{dI_g}{dt}$ in (9) for a sampling time T by:

$$\frac{dI_g}{dt} = \frac{I_g(k+1) - I_g(k)}{T} \tag{10}$$

Then a discrete time equation for the future grid current (one step ahead) is obtained:

$$I_g(k+1) = \frac{1}{R_g T + L_g}\left(L_g I_g(k) + TV(k+1) - TV_g(k+1)\right) \tag{11}$$

The grid currents $I_g(k)$ are measured and used to predict the value of $I_g(k+1)$. Then a $\alpha - \beta$ coordinates transformation is used for decoupling the two components by:

$$I_g(k+1) = I_{g\alpha}(k+1) + jI_{g\beta}(k+1) \tag{12}$$

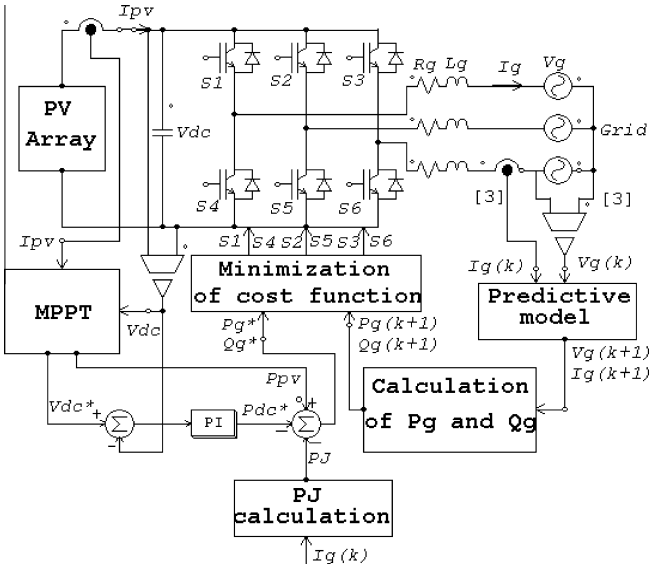

Fig. 10. Proposed predictive power control scheme.

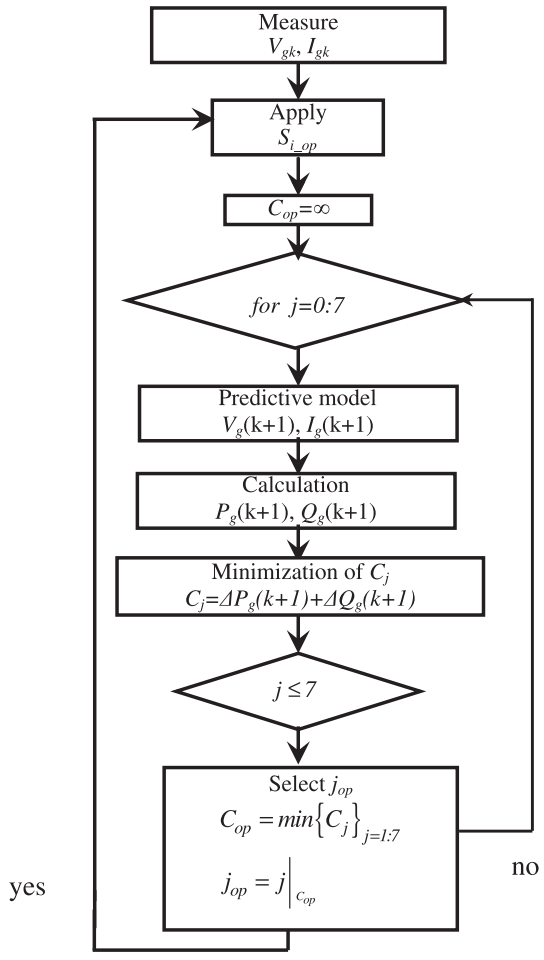

Fig. 11. Flow chart of the predictive algorithm.

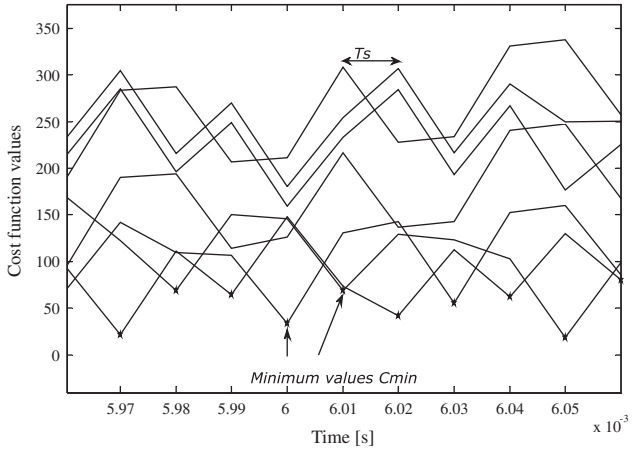

Fig. 12. Cost function optimization.

Table 1
Main simulation parameters.

Parameters	Value	Parameters	Value
C	500 μF	N_s	36
R	0.5 Ω	N_p	2
L	10 mH	V_{gn}	220 V
f	50 Hz	E_g	1.12 V
T	10 μs	A	1.2

5.2. Calculation of P_g and Q_g

These predictions of (11) are used to calculate the future active and reactive power in the grid side, $P_g(k+1)$ and $Q_g(k+1)$ by:

$$\begin{aligned} P_g(k+1) &= V_{g\alpha}(k+1)I_{g\alpha}(k+1) + V_{g\beta}(k+1)I_{g\beta}(k+1) \\ Q_g(k+1) &= V_{g\beta}(k+1)I_{g\alpha}(k+1) - V_{g\alpha}(k+1)I_{g\beta}(k+1) \end{aligned} \tag{13}$$

The reference for active power P_g^* can be expressed as:

$$\begin{aligned} P_g{}^* &\approx P_{pv} - P_{dc}{}^* - P_J \\ P_J &= 3R_g I_g \bar{I}_g \end{aligned} \tag{14}$$

where P_{pv} is the PV array power delivered by the MPPT bloc, P_{dc}^* is the DC link power, $\bar{I}_g$ is the conjugate of I_g current. To regulate the DC link voltage, a PI controller is used that generates the power P_{dc}^* needed to compensate the error in the DC link voltage as it is shown in the proposed control of Fig. 10. Note that P_{dc}^* is more relevant in transients, start up process and for compensate un-modelled losses.

5.3. Minimization of cost function

The cost function C summarizes the desired behaviour of the inverter. As sinusoidal grid currents, in phase with grid voltages are required; the reactive power reference must be zero, $Q_g^* = 0$. The quality function that must be minimized is:

$$C_{[7]} = |P_g{}^*(k+1) - P_g(k+1)| + |Q_g{}^*(k+1) - Q_g(k+1)| \tag{15}$$

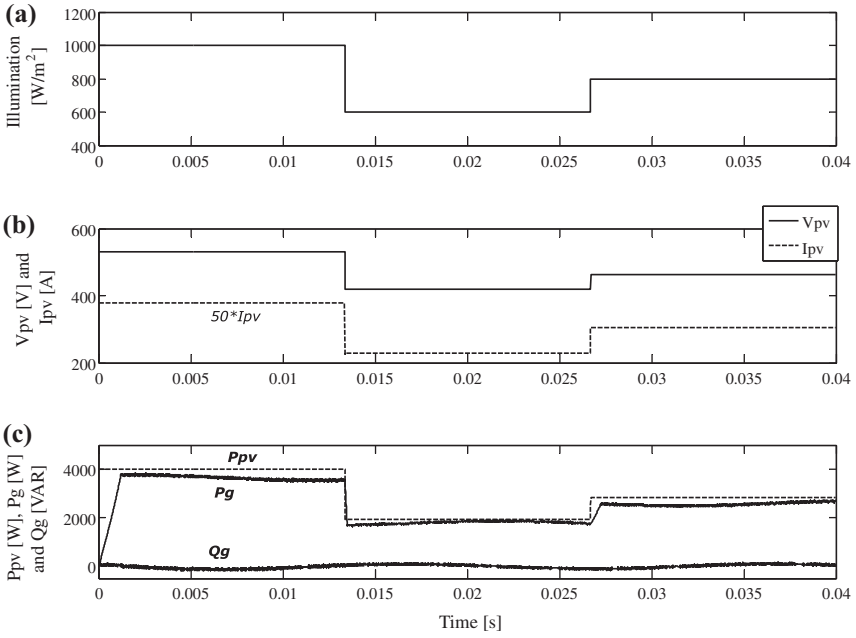

Fig. 13. Simulation results with a two-level inverter configuration (from top to bottom): (a) illumination profile, (b) V_{pv} and I_{pv} (current multiplied by 50) of the PV array, (c) P_{PV}, P_g, Q_g responses for sudden changes of illumination.

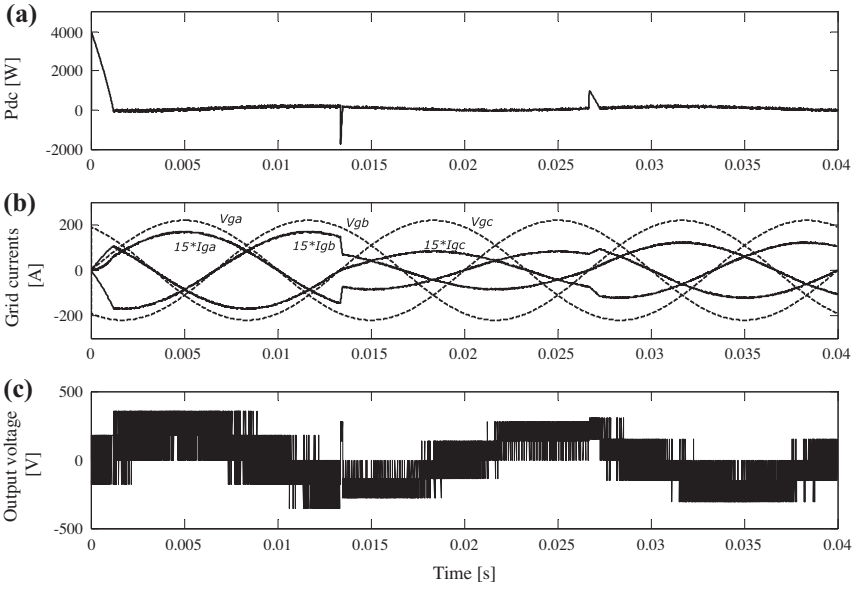

Fig. 14. Simulation results with a two-level inverter configuration (from top to bottom): (a) P_{dc} response, (b) grid currents in phase with grid voltages (currents multiplied by 15) and (c) output voltage of the inverter.

The flow chart of the proposed predictive control is given by Fig. 11, where for each one of the 7 different voltage vectors, the cost function C is evaluated and the voltage vector that minimizes the cost function is then applied during the next sampling period according to the receding horizon control as can be shown in Fig. 12.

The predictive controller is summarized in the next steps:

(1) Measure of voltages and currents of the grid side $V_g(k), I_g(k)$.
(2) These measurements are used to predict grid voltages and grid currents values $V_g(k+1), I_g(k+1)$ for all seven different voltage vectors.
(3) The seven prediction are evaluated using the cost function C of (15).
(4) The optimal switching state that corresponds to the optimal voltage vector that minimizes the cost function is selected to be applied in the next sampling time.

6. Validation of the predictive strategy

The parameters in the scheme of Fig. 10 are given in Table 1.

The simulation has been done in Matlab environment with a step size of 10 μs. Fig. 13 shows the system response when a sudden change of irradiance happens at 0.013 s and again at 0.027 s from 1000 W/m^2 to 600 W/m^2 and then to 800 W/m^2 with temperature at 25 °C. Fig. 13 depicts the power delivered by the MPPT bloc to the system, it can be seen that the system reaches steady state for both illumination levels within the order of few milliseconds The active power P_g, the reactive power Q_g of the grid and the DC link power P_{dc} are clearly decoupled and they are illustrated also in the bottom of Fig. 13. One can see that the reactive power tends to zero for both transient and steady state and it is not affected by the sudden change of irradiation while the active power of the grid P_g has the same profile of the power delivered by the MPPT bloc (P_{pv}) since $P_g^* \approx P_{pv} - P_{dc}^* - P_j$.

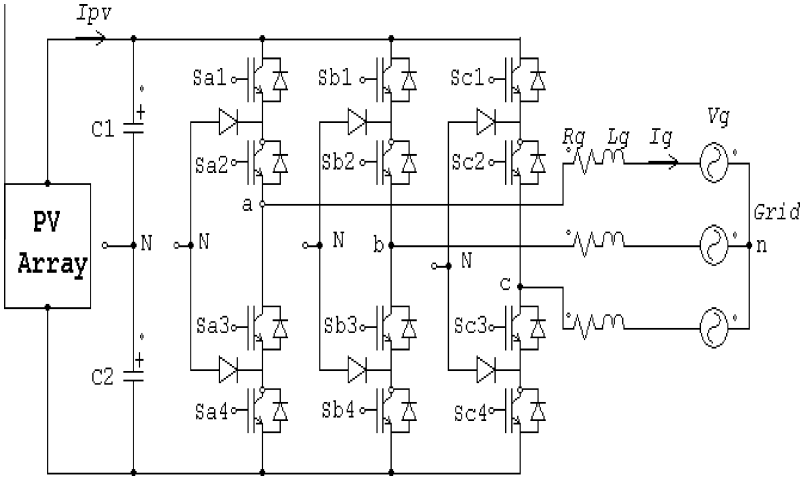

Fig. 15. Three-level NPC converter configuration of the studied system.

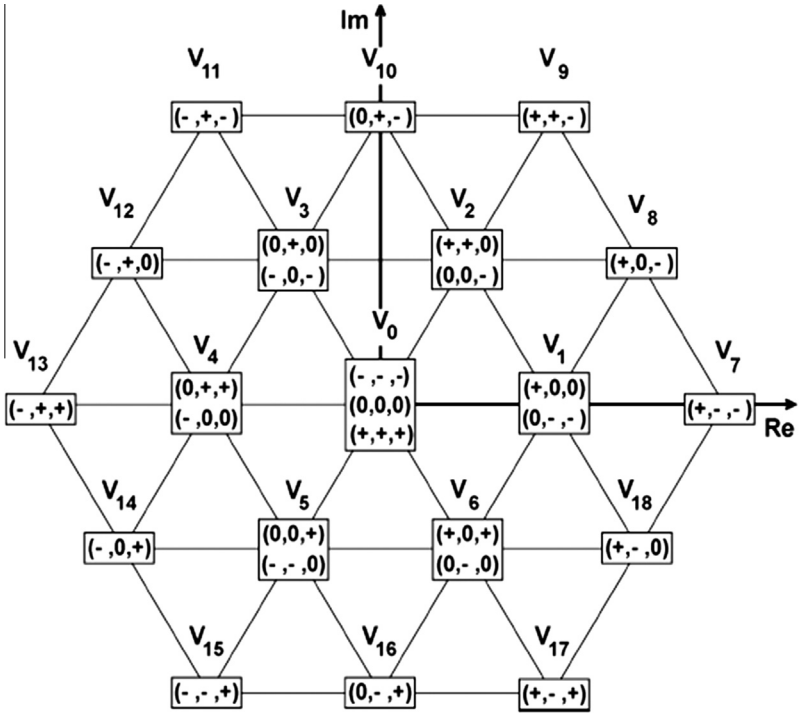

Fig. 16. Possible voltage vectors and switching states generated by a three-level inverter.

Except the steady state, the DC link power P_{dc} is practically zero, being significant only during transients as can be seen in the top of Fig. 14.

Fig. 14 shows that the grid currents and grid voltages are in phase for both illumination levels 1000–600–800 W/m^2 and the fundamental frequency is 50 Hz, also, the grid currents present very good tracking performances with less harmonic distortion.

The above figures show that the instantaneous active power P_g, the reactive power Q_g of the grid side and the DC link power P_{dc} contain an undesirable oscillating part which correspond to an oscillating power term ($\tilde{P}_g, \tilde{Q}_g, \tilde{P}_{dc}$) that flows between the DC link and the RL filter causing supplement harmonics in the grid currents waves and losses in the conversion chain, the instantaneous powers can be decomposed as:

$$\begin{aligned} P_g &= \bar{P}_g + \tilde{P}_g \\ Q_g &= \bar{Q}_g + \tilde{Q}_g \\ P_{dc} &= \bar{P}_{dc} + \tilde{P}_{dc} \end{aligned} \tag{16}$$

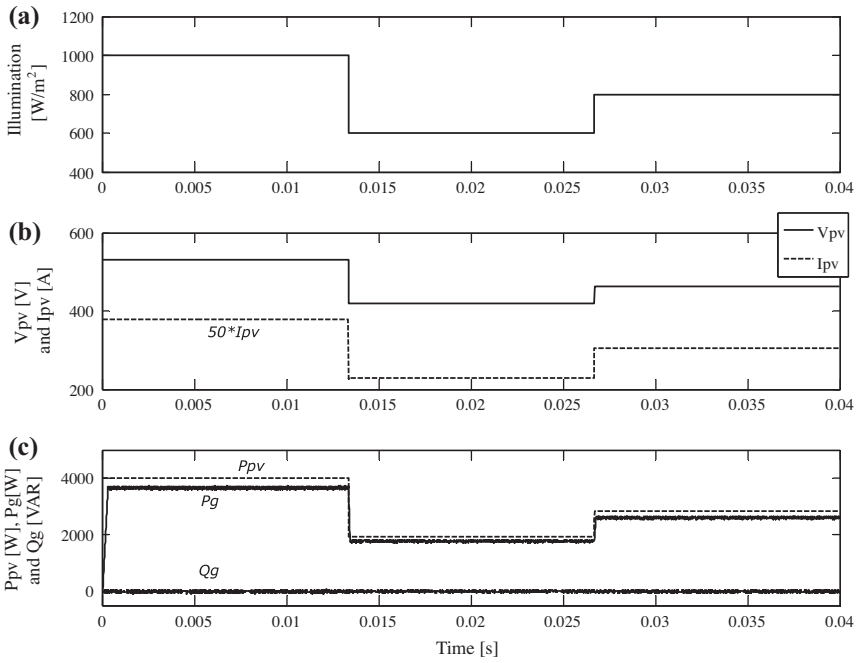

Fig. 17. Simulation results with a three-level inverter configuration (from top to bottom): (a) illumination profile, (b) V_{pv} and I_{pv} (current multiplied by 50) of the PV array and (c) P_{PV}, P_g, Q_g responses for sudden changes of illumination.

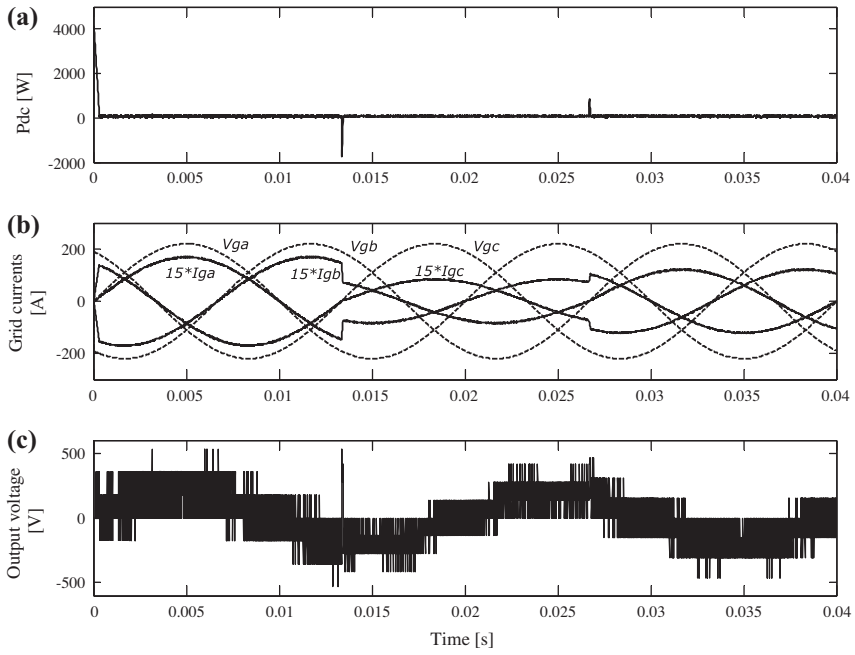

Fig. 18. Simulation results with a three-level inverter configuration (from top to bottom): (a) P_{dc} response, (b) grid currents in phase with grid voltages (currents multiplied by 15) and (c) output voltage of the inverter.

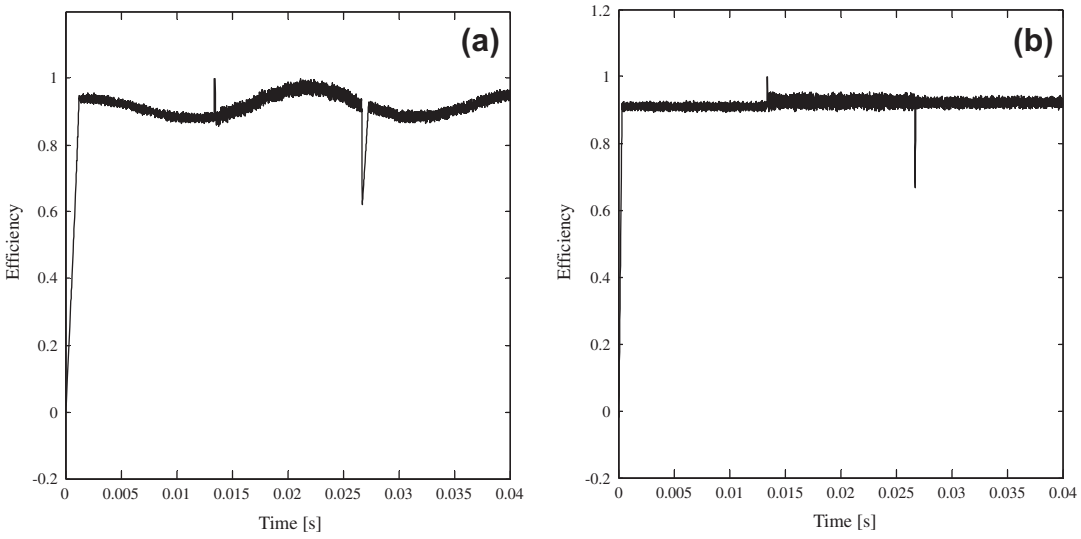

Fig. 19. Efficiency of the conversion chain for the whole cycle: (a) with two-level-inverter structure and (b) three-level inverter structure.

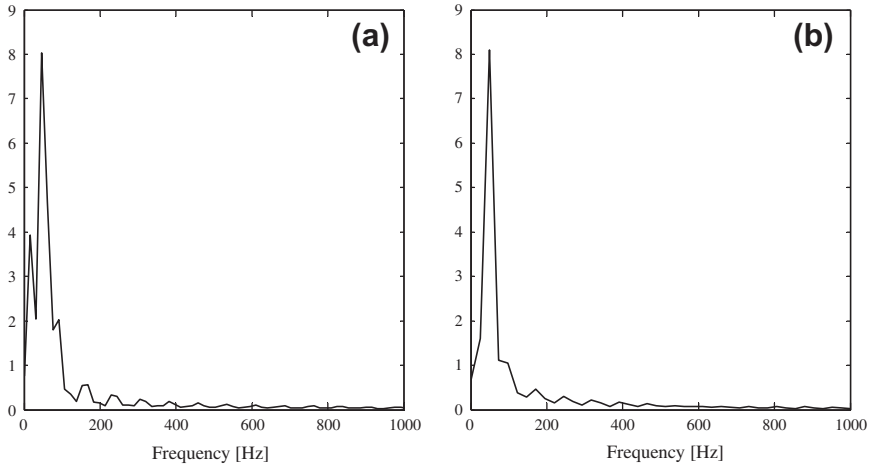

Fig. 20. Spectrum of grid current for the two structures: (a) two-level inverter topology and (b) three-level inverter topology.

7. Predictive power control with three level voltage inverter

To eliminate these oscillating power terms and in order to enhance and improve the obtained results a three-level Neutral Point Clamped NPC inverter considered generally for medium voltage high power applications is used to improve the performance of the studied system. The power circuit is shown in Fig. 15. These kinds of converters have several advantages over the traditional two-level converters, such as, operation with voltages over the switching devices rating, reduced common-mode voltages and smaller voltage changes (dv/dt). Note that the voltage balance of the DC link capacitors is not considered here. The converter applies to the load 19 voltage vectors, which are generated from 27 switching states, as presented in Fig. 16.

The quality function to be minimized for 27 voltage vectors now is given by:

$$C_{[27]} = |P_g * (k+1) - P_g(k+1)| + |Q_g * (k+1) - Q_g(k+1)| \quad (17)$$

Let us examining now the results obtained with a three-level voltage source inverter topology simulated with the same parameters of Table 1. The results are given by Figs. 17 and 18 where a significant difference appears by the disappearance of the oscillating power components ($\tilde{P}_g, \tilde{Q}_g, \tilde{P}_{dc}$) and fast dynamic response is obtained for the grid active power P_g and the DC link power P_{dc} compared to those with a two-level inverter configuration.

The efficiency of the conversion chain can be viewed as the ratio between the active power of the grid to the photovoltaic power given by the MPPT bloc by:

$$\eta_{ch} = \frac{P_g}{P_{PV}} \quad (18)$$

By observing Figs. 19 and 20, we confirm that the performances of the studied system with three-level configuration are highly improved since the power oscillating term is eliminated with very good tracking performances in front of sudden change of irradiance levels, high efficiency of the conversion chain is obtained, the grid currents are in phase with the grid voltages and low harmonic distortion for the line currents is obtained around 1.78%. As a conclusion we can see that the main objectives cited above are fulfilled and the solar energy is transferred efficiently to the utility grid since the MPP is tracked accurately and rapidly and unity power factor in the grid side is reached with high performance and low harmonic distortion.

8. Conclusion

An improved control strategy is proposed to control efficiently a grid connected photovoltaic conversion chain.

The method uses firstly a predictive control associated with a two-level three phase inverter to validate the control strategy, then a three-level converter is used to improve and highlight the results. The predictive approach uses the discrete nature of the power converter and generates sinusoidal grid currents with unity power factor in the grid side without any type of controllers or modulators. The controlled active and reactive power are highly decoupled.

The results show that predictive control is very powerful method since it provides good tracking property and shows high performance. The method is an attractive tool with a conceptually different approach than PWM and SVM modulation to control power converters.

References

[1] Xiao W et al. A modified adaptive Hill climbing MPPT method for photovoltaic power systems. In: Proceedings of the 35th annual IEEE power electronics specialists conference Aachen, Germany; 2004. p. 1957–63.
[2] Koutroulis E et al. Development of a microcontroller based photovoltaic maximum power point tracking control system. IEEE Trans Power Electron 2001:46–54.
[3] Hua C et al. An on line MPPT algorithm for rapidly changing illuminations of solar arrays. Renew Energy 2003;28:1129–42.
[4] Femia N et al. "Optimization of perturb and observe MPPT method". IEEE Trans Power Electron 2005;20:963–73.
[5] Kuo YC et al. Novel maximum power point tracking controller for photovoltaic energy conversion system. IEEE Trans Ind Electron 2001;48:594–601.
[6] Yu GJ et al. A novel two-mode MPPT control algorithm based on comparative study of existing algorithms. Sol Energy 2004;76:455–63.
[7] Lalili D et al. Input output feedback linearization control and variable step size MPPT algorithm of a grid-connected photovoltaic inverter. Renew Energy 2011;36:3282–91.
[8] Song Kim Il et al. New maximum power point tracker using sliding mode observer for estimation of solar array current in the grid connected photovoltaic system'. IEEE Trans Ind Electron 2006;53(4).
[9] Chu Chen Chi et al. Robust maximum power point tracking method for photovoltaic cells: a sliding mode control approach'. Sol Energy 2009.
[10] Felix A. Farret and godoy simoes", integration of alternative sources of energy". USA: Jhon Wiley and sons Inc. publication; 2006.
[11] Zhou Yi et al. Operation of grid-connected DFIG under uunbalanced grid voltage condition. IEEE Trans Energy Convers 2009;24(1).
[12] Castilla Miguel et al. Linear current control scheme with harmonic compensator for PV inverters'. IEEE Trans Ind Electron 2008;55(7).
[13] Carlos Meza et al. Boost Buck inverter variable structure control for grid connected photovoltaic systems with sensorless MPPT. In: IEEE ISIE conference, Dubrovnik Croatia; June 20–23 2005.
[14] Teodorescu R et al. A new control structure for grid connected LCL PV inverters with zero steady state error and selective harmonic compensation. In: Applied power electronics conference and exposition, APEC'04, vol. 1; 2004.
[15] Rodrıguez J, Pontt J, Silva C, Salgado M, Rees S, Ammann U, et al. Predictive control of three-phase inverter. Electron Lett 2004;40(9).
[16] Cortés Patricio, Rodríguez José, Quevedo Daniel E, Silva Cesar. Predictive current control strategy with imposed load current spectrum. IEEE Trans Power Electron 2008;23(2).
[17] Cortes P, Miranda H, Yuz Juan I, Rodriguez J. Predictive torque control of induction machines based on state-space models. IEEE Trans Ind Electron 2009;56(6).
[18] Vargas R, Cortés P, Ammann U, Rodríguez J, Pontt J. Predictive control of a three-phase neutral-point-clamped inverter. IEEE Trans Ind Electron 2007;54(5):2697–705.